Renewable Energy 241 (2025) 122335

Contents lists available at ScienceDirect

Renewable Energy

journal homepage: www.elsevier.com/locate/renene

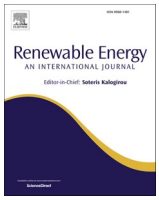

Optimal phasing of tidal stream power around the British Isles and within the English Channel for green ammonia production

Honora Driscoll, Nicholas Salmon, Rene Bañares-Alcántara *

University of Oxford, Department of Engineering Science, Parks Road, Oxford, OX1 3PJ, UK

ARTICLE INFO

Keywords:
Tidal stream energy
Tidal phasing
Green ammonia
Hydrogen carrier
Genetic algorithm
Optimization

ABSTRACT

Green ammonia, a fertilizer, energy carrier and shipping fuel, is a key zero-carbon chemical for the transition to net zero, but is produced in minimal quantities today, predominantly from wind and solar renewable energy. The waters around the British Isles and within the English Channel contain immense potential for predictable tidal stream energy, which is vastly underutilized today. The Haber-Bosch reactor, which is used to produce ammonia, is not flexible, requiring a smooth (consistent) power input. This paper analyses the potential for exploiting the difference in phase of tidal stream currents (tidal phasing) in different locations to optimize the aggregate power profile for the purpose of green ammonia production. A genetic algorithm is used to optimize the location of the turbines. For the four regions analysed in 2050, phasing is always beneficial – the levelized cost of ammonia (LCOA) is reduced by 6–13 % compared to an unphased, single turbine of the same capacity factor (CF), excluding cabling costs. Phasing is particularly evident in the Bristol Channel and in Alderney as their phased power profiles have infrequent zero or low power values. Although the cabling costs are significant, the tidal capital cost (CAPEX) always contributes more than the cabling CAPEX to the LCOA.

1. Introduction

Ammonia is predominantly used for fertilizer applications. New uses of ammonia such as power generation, as a shipping fuel, and as a hydrogen carrier, as well as an increase in population, will markedly increase global ammonia demand to 688 Mt in 2050 (estimated under a 1.5° scenario) from 183 Mt in 2020 [1]. However, current ammonia production methods are not sustainable, with near exclusive production from fossil fuels (i.e. natural gas, coal, heavy fuel oil and naphtha) and negligible production from renewable energy (green ammonia). Conversely, a global green ammonia production capacity of 566 Mt is expected in 2050 (1.5° scenario), i.e. 82 % of global ammonia demand in 2050. Planned green ammonia production is dominated by solar and wind but there is no existing or planned green ammonia production from tidal stream energy or tidal range energy [1], despite its desirable predictability.

A flat power profile is the most ideal profile for green ammonia production as oversizing of equipment can be avoided, and no energy storage or hydrogen storage would be required (unless the capacity factor, CF, is exceptionally low). Moreover, the Haber-Bosch (HB) process is not flexible [2], so the less variable the power profile, the more efficiently the HB can operate. A flat power profile is not possible to achieve with renewable energy, with some exceptions (such as hydropower), unless an external storage component is incorporated. For example, utilising (unphased) tidal stream energy with storage such as flywheels or vanadium flow batteries [3–5] or utilising the grid to back-up renewable energy sources [6]. The issue with using tidal energy with external storage or the grid is the added costs of the, albeit predictable [3], storage capacities and grid connection. Moreover, if the grid is not powered by renewables, the emissions associated with utilising the grid could be substantial. Furthermore, grid emission intensities are highly spatio-temporally variable [7].

A smooth (consistent) power profile with a degree of baseload power is a more realistic profile which could be achieved with renewable energy (without external storage) and would still be useful for green ammonia production. This can be achieved, for example, by exploiting the difference in phase of tidal stream currents in different locations [8–15] or utilising tidal stream energy and tidal range energy together (as they can have a relative phase difference) [16,17]. Combining other renewables, such as solar and wind can increase the capacity factor compared to either resource alone [16], but baseload power is not guaranteed, given the inherent variability and unpredictability of these

* Corresponding author.
E-mail address: rene.banares@eng.ox.ac.uk (R. Bañares-Alcántara).

https://doi.org/10.1016/j.renene.2024.122335
Received 14 April 2024; Received in revised form 19 November 2024; Accepted 31 December 2024
Available online 8 January 2025

resources. However, the power profile from tidal stream and tidal range energy can be predicted, and thus, baseload power can be guaranteed. Moreover, although tidal stream and tidal range energy are green solutions to providing baseload power, tidal range energy has notable environmental issues such as fish migration [18,19]. Thus, exploiting the difference in phase of tidal stream currents in different locations, i.e. tidal phasing, is an attractive option to provide power for green ammonia production.

It is known that tidal phasing increases the minimum power and decreases the maximum power [15], making the power profile less variable. It could be argued that, with infinite phasing, the power profile would be flat with respect to time. Fig. 1 shows four theoretical power profiles with the same capacity factor – from a single turbine, from two turbines, from 10 turbines and the ideal flat profile (from an infinite number of turbines). Capacity factor is defined as the mean power in a time frame compared to the rated power, with a maximum value of 1 and a minimum value of 0. The capacity factor depends on various parameters such as the velocities of the tidal stream currents, the type of turbine and the location of the turbine in the water column. The power profiles represent an M2 tidal power profile with a period of 12.42 h and incorporate arbitrary cut-in and rated speeds (0.2 m/s and 0.9 m/s). M2 is the semi-diurnal lunar tidal constituent, which is the most important tidal constituent for the British Isles [17].

The phased profiles are less variable than the unphased (single-turbine) profile. Moreover, more phasing ensures that the power profile is closer to the ideal flat profile. Using these four power profiles as input power to a green ammonia plant will result in very different LCOAs with the flat profile being the lowest and the single-turbine profile being the highest.

The HB process power requirement is a small fraction of the total power of the green ammonia plant (<5 %), and the minimum power of the HB is about 20 % of its rated power [2] (i.e. < 1 % of the total power of the ammonia plant). One also has to consider that to keep the HB at a minimum load, there is an associated minimum hydrogen supply requirement. Depending on the power profile at any given time, this hydrogen supply requirement may be sourced directly from the electrolyser or from hydrogen storage. Thus, the power requirement associated with the minimum hydrogen supply as a reactant to the HB varies with time. Phasing could ensure that the power profile always meets the minimum power of the HB (from input power directly, avoiding extra battery or fuel cell capacity) as well as the minimum hydrogen supply requirement, providing confidence to manufacturers and investors.

The authors were the first to study green ammonia production utilising tidal stream energy [20], and the first to study green ammonia production utilising tidal phasing (with case studies in Orkney and the Irish Sea) [8]. The tidal phasing study chose complementary tidal locations based on correlation coefficients which successfully reduced the LCOA by up to 11 %. This paper extends on the tidal phasing study in four aspects. Firstly, incorporating optimization of the aggregate power profile by selecting appropriate locations of tidal turbines i.e. automatically choosing turbine locations, rather than choosing them manually through correlation coefficients. Secondly, utilising a larger region, i.e. the waters around the British Isles and within the English Channel, rather than two case studies within this region. Thirdly, incorporating 2050 CAPEX costs. Fourthly, incorporating a turbine spacing constraint and accounting for power reductions from wake and blockage effects.

There are only two academic papers which optimize the location of tidal stream turbines to optimize the aggregate power profile by exploiting complementary phase differences – Neill et al. [17] and Giorgi and Ringwood [21], from 2014 to 2013 respectively. Giorgi and Ringwood [21] utilise a genetic algorithm over 11 locations around the island of Ireland, and Neill et al. [17] utilise a greedy algorithm over the northwest European shelf seas. Our work utilises smaller regions than in

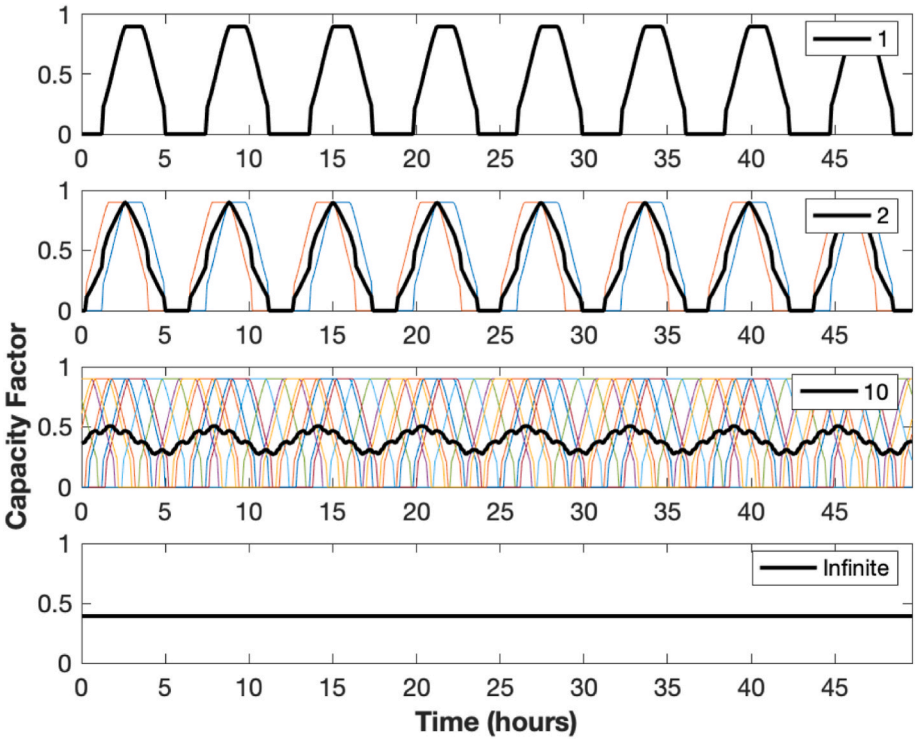

Fig. 1. Theoretical power profile from a single turbine, two turbines with a phase difference of 1 h, 10 turbines with a phase difference of 1 h each and an ideal power profile representative of an infinite (very large) number of turbines. The four power profiles in black have the same capacity factor (39 %). The non-black power profiles are the individual turbine power profiles. The free stream velocity is estimated as $\sin\left(\frac{2\pi}{12.42}(t+p)\right)$, where t is time in hours and p is phase difference in hours.

Ref. [17] or [21], and utilises tidal energy for green ammonia production, rather than for the grid. Improvements of our work with respect to Refs. [17,21] include: i) using all water depths above the minimum operable turbine water depth (not constrained to 25–50 m as in Ref. [17]), since we consider floating turbines which can operate in deep water [22], and ii) no restriction on the minimum velocity (a minimum M2 current of 1.5–2.5 m/s is used in Ref. [17], and a minimum tidal current velocity of 2.0 m/s is used in Ref. [21]).

Orkney, an archipelago in the North of Scotland, has some of the best tidal stream energy in the world [23]. However, even with the new 220 MW transmission link from Orkney to mainland Scotland (Caithness) [24], Orkney is grid-constrained. Orkney has a large surplus of tidal stream energy (and wind energy) that cannot be used within the archipelago as it is sparsely populated [25,26]. Thus, producing green ammonia from tidal stream energy in Orkney facilitates the utilisation of otherwise unexploitable tidal energy.

It is acknowledged that tidal phasing is not a unique phenomenon. Regen (an independent centre of energy expertise) demonstrated the benefits of utilising offshore wind on both the east and west coast of the UK [27]. Similar to tidal phasing, strategically placing wind turbines apart to utilise power profile anti-correlation (in different weather windows) can facilitate less variable and more consistent power generation.

2. Methodology

The process of selecting regions, modelling tidal stream turbines, selecting turbine locations, and costing green ammonia production is explained in this section, aided by Fig. 2.

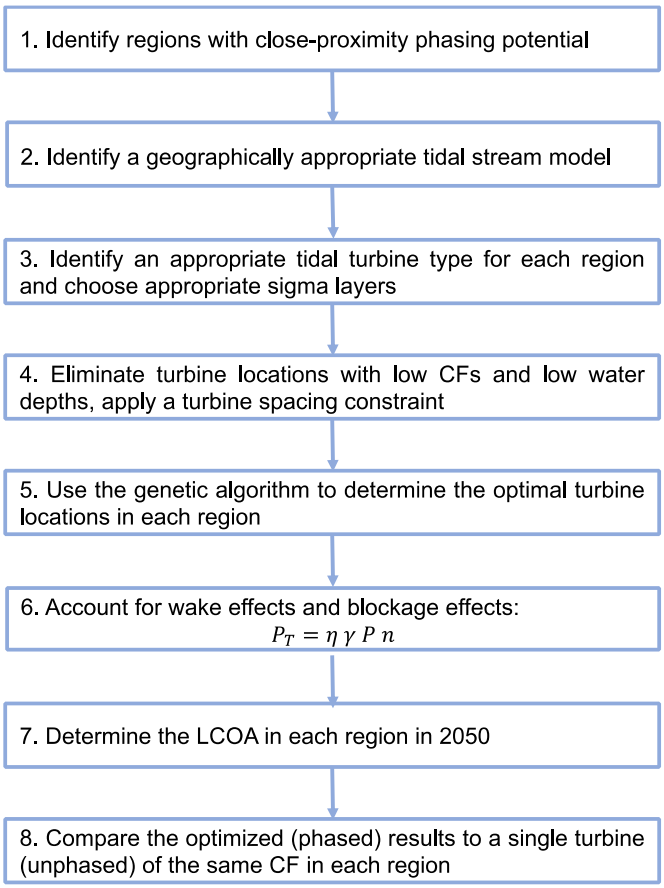

Fig. 2. Flow diagram of the methodology.

1. Identify regions in the waters around the British Isles and within the English Channel with both close-proximity tidal phasing potential and high-energy tidal potential by analysing tidal current phasing maps [10,17]. Identify an onshore location that is suitable for a green ammonia plant in each region (i.e. on grassland [28] and avoiding protected land [29]). The results from this step are shown in Fig. 3.
2. Identify a geographically appropriate tidal stream model. The Scottish shelf model (SSM) climatology version 2.01 [30], the Pentland Firth and Orkney waters (PFOW) model climatology version 1.02 [31,32], and the Firth of Clyde (FOC) model climatology version 1.03 [33] provide 3D tidal stream velocities at hourly and high spatial resolution. The PFOW and FOC models are part of the SSM but the PFOW and FOC models have a higher spatial resolution than the SSM. The PFOW model has been used in other tidal stream energy studies, such as [32]. Tidal hotspots that do not lie in the PFOW and FOC models are covered by the SSM (such as the English Channel).
3. Identify an appropriate tidal turbine type for each region. The Orbital O2 turbine, a floating, 2 MW, two-bladed, horizontal axis, two-rotor, 20 m diameter turbine, is used in all regions with a minimum operable water depth >23.2 m [34]. The cut-in speed is 1 m/s, the rated speed is 2.5 m/s, and the cut-out speed is 4.5 m/s [34]. For shallow regions, the 0.28 MW PLAT-I device (a smaller, floating, three-bladed, horizontal axis, four-rotor, 6.3 m diameter turbine) is used, which has a minimum operable water depth of 10 m [26]. For low-energy regions, the 0.28 MW PLAT-I device is also used, as it has a low cut-in speed of 0.5 m/s [35], enabling more hours of non-zero energy production. The rated speed is 2.7 m/s, and the cut-out speed is 4 m/s [26]. The method of converting the hourly velocities at each location within the SSM, PFOW model and FOC model to hourly power values was followed from Appendix B of [20]. Velocities are selected at sigma layers (vertical layers) appropriate for the turbine's location in the water column in each region. The number of sigma layers is selected based on the vertical distance that the turbine fills in the water column. That is, the diameter of the turbine relative to the mean lowest water depth in each region (displayed in Table 1). Since the turbines modelled are floating, sigma layers close to the top of the water column are chosen (low sigma layer values). The 3-D tidal stream velocities are larger near the top of the water column (near the surface) and lower near the bottom of the water column (by the seabed). The turbines will be most efficient at lower sigma layers. Since each region has a different water depth, the specific water depth for the highest turbine efficiency will vary for each region.
4. Individual turbine locations are restricted to capacity factors above 0.15 (which is the lower CF limit in Ref. [15]). All turbine locations with minimum water depths <10 m are discarded. When the Orbital O2 turbine is used, turbine locations with minimum water depths <23.2 m are discarded in that region (Table 1). From an order of magnitude perspective, phasing will only be beneficial if the capacity factors of the turbine locations considered are similar. Thus, the green ammonia plant in each region incorporates phased turbine locations with $0.15 < CF < 0.3$. A turbine spacing of 2.5D lateral by 10D downstream [36] is applied (D is diameter) which is the European Marine Energy Centre's (EMEC) suggested tidal turbine spacing.
5. Determine the optimal turbine locations in each region. To optimize the aggregate power profile, P, the optimal turbine locations are chosen (depending on their location-specific power profiles) to maximise an objective function using the genetic algorithm in MATLAB. The input power profiles (to the optimization model) are ranked from the highest annual capacity factor to the lowest. The optimization model is given k individual power profiles, and the optimization model will choose n ($n \leq k$) power profiles that, combined, give the optimal aggregate power profile, P. The objective function, f, is to maximise the mean power magnitude, P_m, and minimize the time, T_λ, that the power profile, P, spends below a given fraction, λ, of the mean power.

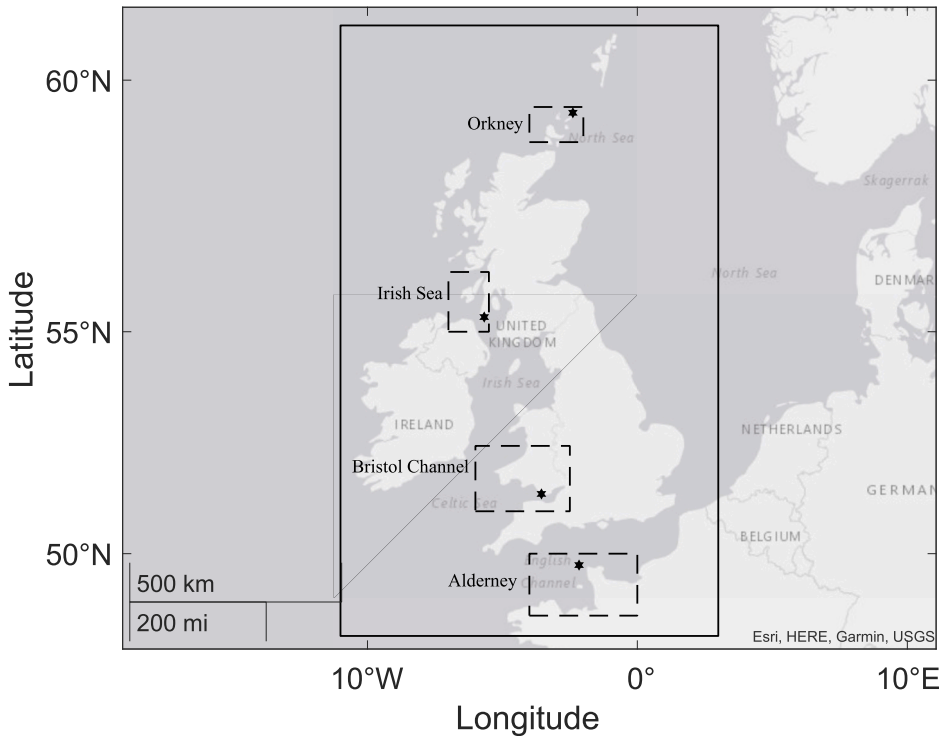

Fig. 3. Four tidal regions with close-proximity tidal phasing potential and high-energy tidal potential and associated ammonia plant locations (black hexagrams). The solid line represents the domain considered.

Table 1
Tidal stream turbine modelling details. Tidal regions correlate with Fig. 3, top-down, north to south).

Tidal region	Tidal model	Mean lowest water depth in region (m)	Tidal turbine type	Sigma (vertical) layers	Water depths used	Power capacity modelled (MW)
Orkney (excluding the Pentland Firth)	PFOW	44.2	PLAT-I	2–3 out of 10	>10 m	1332
North Channel of the Irish Sea	FOC	48.3	Orbital O2	2–5 out of 10	N/A	1980
Bristol Channel & Pembrokeshire	SSM	49.2	PLAT-I	2–4 out of 20	>10 m	187
Alderney	SSM	53.5	Orbital O2	2–9 out of 20	>23.2 m	4316

$$f = \max\left[P_m(T - T_\lambda)\right]$$

In this analysis, λ is taken as 0.3, which is the upper-end of the value used in Ref. [17]. The objective function is the same as in Neill et al. [17], but the time period, T, for optimization is 29.5 days (2 spring-neap cycles [15]) rather than 12.42 h (period of the semi-diurnal lunar constituent, M2). To ensure that the optimization algorithm has a choice of turbine locations, the number of turbine locations, n, is fixed at 25 % of the maximum (the maximum number of turbine locations, k, is all locations with CF > 0.15 in that region). The optimal aggregate power profile, P, over a year, is:

$$P = \frac{\sum_{i=1}^{i=k} P_i L_i}{P_{max} \sum_{i=1}^{i=k} N_i L_i}$$

P_i is the power profile over one operational year (365 days minus 14 days for maintenance [6]) at each turbine location, *i*. L_i is the location identifier parameter, with a value of either 0 or 1, and $\sum_{i=1}^{i=k} L_i = n$. If $L_i = 0$, the corresponding turbine location is not utilized. If $L_i = 1$, the corresponding turbine location is utilized. The genetic algorithm chooses the values of L_i to maximise f. The denominator normalizes P, so it's highest value is 1 and lowest is 0. P_{max} is an individual turbine's power capacity (2 MW or 0.28 MW). N_i is the number of turbines per location. The optimal turbine locations are shown in Fig. 5. L_i has a size of k, so the number of variables to be optimized is k. The starting point for L_i is 1 for the highest n capacity factor turbine locations and 0 for all other turbine locations.
Default MATLAB genetic algorithm parameter values were used – the maximum number of generations is 100k, the population size is 200, the stopping condition function tolerance is 10^{-6} over 50 generations, and the crossover fraction is 0.8. The convergence time in each case was less than 1 h.

6. The total power from a tidal farm, P_T, will be affected by wake effects and blockage effects [37] which will lower P_T by η and γ respectively. Therefore, $P_T = \eta\,\gamma\,P\,n$, where P is the rated power of an individual turbine and n is the number of turbines in a farm. Blockage effects in this paper refer to the reduction in tidal stream velocity as the flow approaches the turbines (the blockage). Wake effects refer to the reduction in tidal stream velocity downstream of the turbines. The same blockage and wake correction factors are applied to all turbines in the array (spatially constant coefficients). This is an approximation to account for a lowered power output with turbines present compared to no turbines present. Two parameters (η and γ) are incorporated to highlight that two separate power reduction processes are occurring. η, the wake loss, is around 0.90–0.95 [38,39]

for a wind farm, and η is approximated as 0.90 for all tidal farms in this paper. It is acknowledged that the fluid flow behavior will differ in a tidal stream turbine farm compared to a wind farm [40,41]. However, due to the lack of deployment of tidal turbines compared to wind turbines [25], and the complexity of modelling wake effects from tidal turbines [42], wake effect assumptions are drawn from wind farms in this paper. γ, the blockage loss, is approximated as 0.87, based on field data from the MeyGen project (four, 1.5 MW turbines with a capacity factor of 34 % generated 21 GWh in 18 months of operation [43] where $\eta \times \gamma$ is 21 GWh/(0.34 $\times$ 18 months $\times$ 6 MW)). It is acknowledged that γ is site dependent and will vary depending on a number of parameters such as the number of tidal constituents used in modelling the tidal stream velocity, water depth, turbine spacing, size of turbine, and bed friction [37,44]. It is out of the scope of this paper to determine an accurate power profile accounting for the interaction between all turbines in the arrays in each region analysed, as this would be very computationally expensive, and also a research area under development. Moreover, there is very little publicly available data on power production from operating tidal stream arrays. It should be noted that Neill et al. [17] and Giorgi and Ringwood [21] did not explicitly incorporate wake effects or blockage effects in their modelling of tidal energy.

7. The optimized hourly tidal stream power profile is inputted to a mixed integer linear program (MILP) green ammonia production optimization model [6] to determine the minimum levelized cost of ammonia (LCOA). Cable costs, equipment capital costs (CAPEX) and operating costs (OPEX) are incorporated into the cost model (shown in Table A.1 in the Appendix). 2050 costs are used as the deployment of tidal stream turbines is only around 10 MW in the UK today [25] and this work models tidal capacity much larger than 10 MW (7815 MW; Table 1), which would be unrealistic today but not in 2050. The main point of this paper is to determine the reduction of the LCOA due to phasing - a similar LCOA reduction due to phasing would be expected using today's costs. The climate scenario considered for the equipment costs is RCP 2.6 as it is an ambitious climate scenario, and the tidal stream capacity modelled is also ambitious. It should be noted that sea-level rise effects are not incorporated into the tidal stream velocities.
8. Compare the optimized (phased) power profile and its LCOA (and equipment capacities) to a single (unphased) turbine of the same yearly capacity factor. Cable costs are excluded for a fair comparison as the optimized case represents a much larger power capacity compared to the single turbine. Then, for the phased power profiles, include the cable cost in the LCOA and compare the equipment CAPEX and OPEX contributions to the LCOA to see if the cabling is significant.

3. Results and discussion

3.1. Tidal regions

The results from steps 1–4 of the methodology are shown in Table 1 and Fig. 3. The four regions with close-proximity tidal phasing potential, and high-energy tidal potential are Orkney, the North Channel of the Irish Sea, the Bristol Channel & Pembrokeshire and Alderney. This work expands upon first-generation tidal sites [9] and tidal sites used in other tidal phasing papers [10,17], with the case of the Bristol Channel (which has tidal sites deeper than 50 m). The four regions exclude Anglesey, the Isle of Man and the Isle of Wight due to their relatively large distance from other tidal sites and lack of complementary phase difference with surrounding tidal sites. Moreover, no tidal sites on the east coast of the UK were chosen due to the lack of both phasing and tidal power potential. The Pentland Firth is excluded from this analysis, due to its limited phasing potential [8,13] and its exceptional tidal resource [44] which would already likely yield low LCOAs if utilized alone (i.e. without incorporating phasing from other regions).

The power capacities proposed in each region are checked against the technically unconstrained power capacity limits (detailed in Ref. [9]), and ensured to be lower than these limits, although not all turbine locations in this paper appear in Ref. [9]. There is uncertainty in the technically unconstrained power capacity limits, so this power comparison is approximate. Detailed modelling of the technically unconstrained power capacity limits in each region would be beneficial. The power capacities modelled are displayed in the last column of Table 1, entitled 'Power capacity modelled (MW)'. It is acknowledged that the power capacities modelled are high compared to around 10 MW of tidal stream turbine deployment in the UK today [25]. However, to put these capacities in context, 11.5 GW is the UK and British Channel Island's practical tidal stream resource potential [25]. With the very low tidal stream turbine deployment today, it is unknown whether the UK could manufacture and deploy tidal capacity on a scale two or three orders of magnitude higher by 2050. However, this analysis is beyond the scope of this paper.

Two modifications to the methodology are required. i) As in Ref. [8], all water depths are included in the FOC model, to ensure that the Sound of Islay (within the Irish Sea case study) is included, as it has significant phasing potential. This modification only affects the Irish Sea case study. ii) Due to the large number of high-energy turbine locations in Orkney, and to avoid modelling an unrealistically large number of turbines, the turbine spacing in Orkney was altered to ten times the spacing used in the other regions (2.5D lateral by 10D downstream [36]).

3.2. Phasing results

The results from steps 5–8 of the methodology are presented in this section.

3.2.1. Tidal phasing benefits and drawbacks

In each region, the phased (optimized) power profile is less variable than the unphased power profile (from a single turbine of the same yearly capacity factor), meaning that the phased power profile resides mostly in moderate power values (Fig. 4 left). Phasing is particularly evident in the power profiles for Bristol and Alderney which are infrequently at zero or low power values. It should be noted that η and γ are not applied to the single location's power profile, as it is a single, isolated turbine. In each region, the turbine locations utilized by the optimization model are spread out to incorporate phasing (Fig. 5). If there were no complementary phase differences to exploit by utilising turbines in different locations, there would be no LCOA reduction (Fig. 4).

The comparison between green ammonia production using a phased power profile and an unphased power profile (from a single turbine of the same yearly capacity factor), is used to show how phasing affects the equipment CAPEX in each region. Compared to the unphased power profiles in each region, the phased power profiles have a reduced LCOA, tidal CAPEX, electrolyser CAPEX, HB + ASU CAPEX and energy storage CAPEX in 2050 (Fig. 4 right). The phasing benefit is significant, as the LCOA is reduced by 6–13 %. In each region, the energy storage CAPEX has the largest reduction (50–85 %) of all the equipment CAPEX reductions. Moreover, the phased power profiles go to zero in every region (albeit with varying frequency), meaning energy storage requirements are not eliminated. It should be noted that the unphased power profile is not the same in each of the four regions, so the region which benefits the most from phasing cannot be determined directly from the LCOA reduction. Moreover, the unphased power profiles will have different characteristics such as mean power, frequency of zero power and coefficient of variance.

Incorporating tidal phasing into green ammonia production has four main operational benefits. These comprise i) less reliance on energy storage to provide the minimum load of the HB process, ii) more consistent ammonia production, iii) lower equipment capacities, and iv) lower inventory improving process safety.

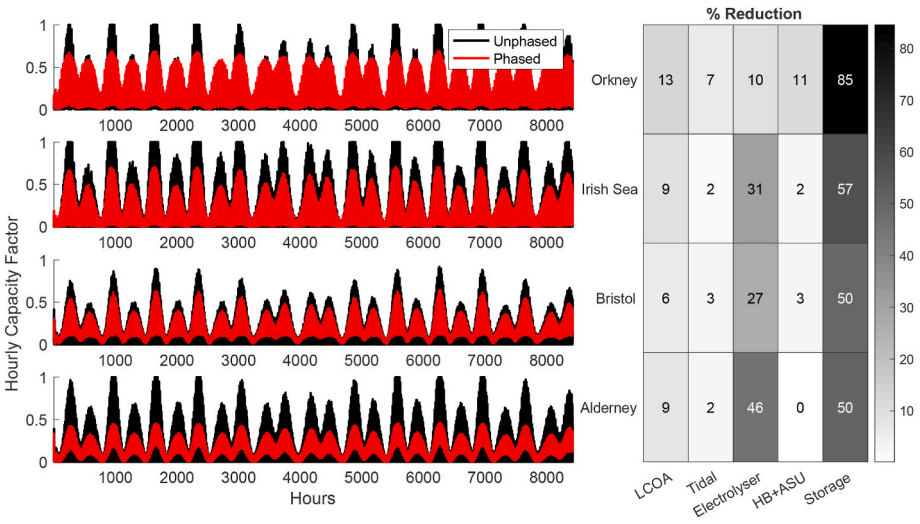

Fig. 4. Left: Power profiles from the optimized, phased turbines and from a single, unphased turbine of the same capacity factor in each region over an operational year (365 days minus 14 days for maintenance). Right: Using these phased and unphased power profiles in each region, the phasing benefit to green ammonia production is displayed as a percentage reduction in LCOA, tidal CAPEX, electrolyser CAPEX, HB + ASU CAPEX and energy storage CAPEX in 2050 (excluding cabling costs). (For interpretation of the references to colour in this figure legend, the reader is referred to the Web version of this article.)

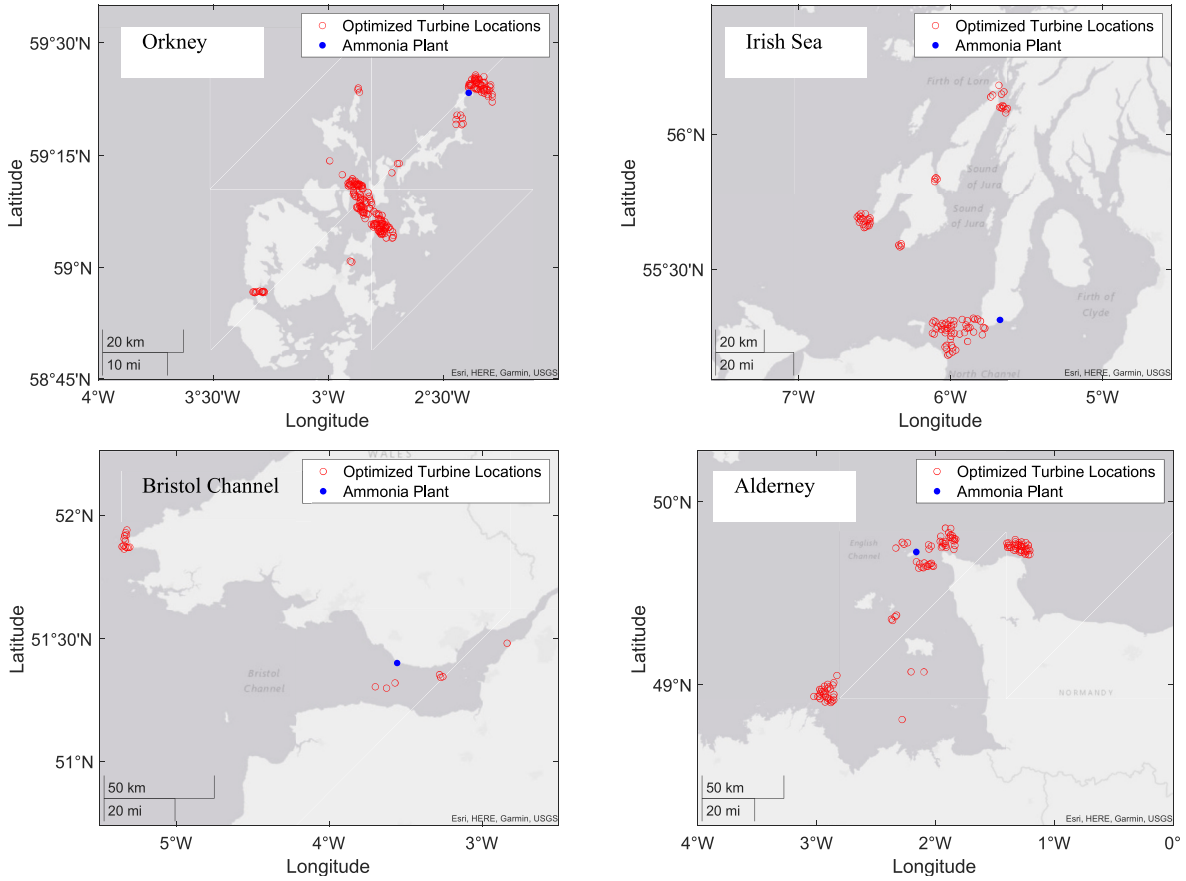

Fig. 5. Turbine locations utilized by the optimization model (in step 5 of the methodology) and associated ammonia plant locations. Each location (red circle) is representative of one or more turbines, the number of which varies depending on the area allocated per location and the EMEC turbine spacing. (For interpretation of the references to colour in this figure legend, the reader is referred to the Web version of this article.)

Firstly, phasing decreases the frequency and duration of low-power periods, which ensures that the minimum load of the HB process is more likely to be met by the input tidal power than by a battery or fuel cell (energy storage). Therefore, the energy storage requirement is reduced ('Storage' column at Fig. 4 right).

Secondly, phasing smooths the power profile, facilitating higher minimum powers and lower maximum powers, providing a less variable power profile over long time periods (Fig. 4 left). This ensures that ammonia production is more consistent, rather than rated ammonia production for a period of time followed by no ammonia production for

another period of time. Consistent ammonia production is attractive to ammonia off-takers, facilitating a consistent shipping schedule to off-load ammonia, which may ease contract initiation and renewal. The number of ammonia storage tanks can be predicted and reduced, avoiding oversized ammonia storage tanks, which would add extra inventory to the plant.

Thirdly, since phasing lowers the maximum power to below the rated power (Fig. 4 left), equipment capacities are less oversized (Fig. 4 right) and thus have a higher load factor than if the maximum power was at rated power. This is particularly important for the electrolyser, which has the largest capacity of the chemical equipment in the plant.

Fourthly, phasing facilitates a simpler ammonia plant, improving process safety since less inventory, that is, smaller equipment and less energy/material storage (Fig. 4 right), is required.

Drawbacks of utilising tidal phasing include: i) optimizing phasing tends to utilise turbines with a lower CF than the highest CF turbines resulting in a high tidal capacity required for a given ammonia production requirement, ii) tidal turbines may be further apart (in Fig. 5) to exploit phase differences (than the highest CF turbines), which requires a longer cable, and iii) optimization modelling (to find the optimal turbine locations) may be computationally expensive and is dependent on the accuracy and resolution of the tidal stream velocity model used.

To incorporate phasing, other objective functions were considered in step 5 of the methodology, such as maximising the minimum power, maximising the mean power and minimising the power variance, as suggested by Giorgi and Ringwood [21]. Maximising the minimum power is not always useful, as some regions will always have a minimum power very close to zero. Moreover, due to the nature of phasing, in regions which can have a minimum power above zero, there is generally a trade-off between a high minimum power and a low mean power and vice versa. Maximising the mean power would not fully incorporate the benefits of phasing, as the locations with the highest mean power may not have phase diversity. Minimising the power variance, by, for example, minimising the sum of the square of errors (where the error is the difference between the power value at each time step and the mean power) or by minimising the coefficient of variation [15] would penalise power values above and below the mean power equally. However, it is preferable to only penalise low power values.

3.2.2. Regional LCOAs

The LCOA in each region in 2050 (with cabling) is shown in Fig. 6 (left) and the relative contribution of equipment CAPEX and OPEX to the LCOA is displayed in Fig. 6 (right). In each region, the largest contribution to the LCOA is from the tidal CAPEX (41–67 %), the cable CAPEX (4–38 %) and the HB + ASU CAPEX (10–17 %). The electrolyser CAPEX (3–7%), OPEX and energy storage CAPEX are smaller contributions to the LCOA. Interestingly, the tidal CAPEX always contributes more than the cabling CAPEX to the LCOA.

The LCOAs in Orkney, the Irish Sea and Bristol are within the range of LCOAs (310–610 USD/t [1]) for conventional green ammonia in 2050 (i.e. ammonia produced using solar/wind, not tidal). Alderney has a particularly large cable cost, so its LCOA is high (803 USD/t). It should be noted that a modelling assumption of one cable per turbine is used, which is a conservative estimate - the actual cable costs would likely be lower.

It is important to stress that lower LCOAs could be obtained from the higher CF tidal locations (CF $>$ 0.3) within the regions analysed. The objective of this paper was not to find the lowest LCOAs from tidal stream energy around the British Isles and within the English Channel but to find small regions where phasing has potential, and to quantify the phasing benefit to ammonia production. It is likely that the highest CF tidal locations (CF $>$ 0.3) will be deployed first, and could be used for green ammonia production, other green fuel production (such as green hydrogen) or grid energy. Producing green ammonia from lower CF tidal locations (CF $<$ 0.3, as in this paper) may enable the utilisation of otherwise unutilized tidal turbine locations.

4. Limitations and future work

Although justified assumptions and modelling decisions were

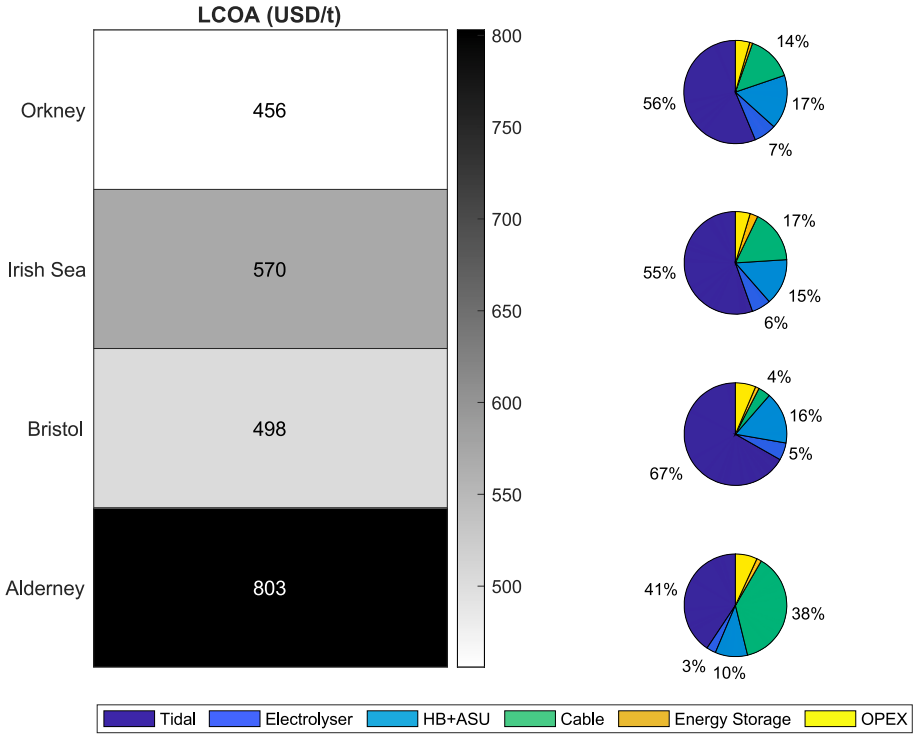

Fig. 6. The LCOA in each region in 2050 (left) and the relative contribution of equipment CAPEX and OPEX to the LCOA (right). The numerical percentage contributions of the energy storage and OPEX are not shown for figure clarity (although they are still represented in the pie chart). Cable costs from the turbines to the onshore ammonia plant (one cable per turbine) are included.

included, further modelling improvements could be incorporated.

Although care was taken to ensure that the CAPEX values are sensible, the CAPEX values have a degree of uncertainty, particularly the tidal CAPEX values (this is acknowledged in the CAPEX justifications in the Appendix). However, the most important result of this paper is Fig. 4, which shows the phasing benefit and the relative LCOA between the unphased and phased scenarios. Thus, the relative LCOA is more informative than the actual LCOA for this analysis. However, future work could apply a sensitivity analysis on the CAPEX and OPEX values to give a range of LCOAs for each year modelled.

This work has incorporated power reductions from wake and blockage effects through the η and γ parameters respectively. The considerable uncertainty of these parameters is already discussed in detail in step 6 of the methodology. However, future work could incorporate collaboration with fluid flow experts to determine, experimentally or computationally, more accurate values of η and γ.

To improve the modelling, additional turbine types (varying in rated power, cut-in speed, diameter and position in the water column – i.e. fixed on the seabed or floating) could be considered for each region or multiple types could be incorporated within a region, as suggested by Novo and Kyozuka [15]. Other modelling improvements include utilising accurate sigma (vertical) layers for the tidal stream velocity at every turbine location (rather than average sigma layers for the region as a whole, Table 1) and incorporating a more conservative minimum operable water depth for each turbine [36]. Moreover, a distance restriction could be applied in the optimization (as suggested in Ref. [17]). This could be used to, for example, minimize the distance between the tidal turbines or minimize the distance between the ammonia plant location and the tidal turbines or both (with the objective of minimising the cable cost).

The precision of the tidal model data is relatively good (as justified below), but higher spatio-temporal resolution tidal velocity and water depth data over more than a year, if available, would provide more credibility to the result that tidal phasing is beneficial for green ammonia production. The tidal model data precision in this work can be compared to the two other optimal-location tidal phasing papers, Neill et al. [17] and Giorgi and Ringwood [21]. This work has i) A high spatial resolution: both [17,21] use the ROMS (Regional Ocean Modelling System) hydrodynamic model to provide tidal stream velocities. In Ref. [21], the horizontal resolution is 1.2 km, and the velocity is depth-averaged. Neill et al. [17] used 11 vertical layers, a longitude resolution of 1/24° and a latitude resolution of 1/32°–1/51°. The SSM, PFOW and FOC models used in our work have a varied spatial resolution of between around 100 m–2000 m [30–33]. The number of vertical (sigma) layers is 20 for the SSM and 10 for the PFOW and FOC models. ii) More tidal constituents: 8 are used in the SSM, PFOW and FOC models [45], compared to one (M2) in Ref. [17] and 4 in Ref. [21]. iii) A lower temporal resolution: velocities have a 10-min temporal resolution in Ref. [21], and the temporal resolution is not stated in Ref. [17]. The SSM, PFOW and FOC models have a temporal resolution of 1 h [30–33].

More advanced power modelling code for tidal turbines would provide a more accurate LCOA. Future work could include a blade element momentum model as well as power fluctuations (such as turbulence or wave loading) and its impact on the LCOA. It should be noted that internal energy storage is incorporated into the model (fuel cell, battery and hydrogen storage), so small power fluctuations likely would not affect the amount of ammonia produced. However, large power fluctuations would likely increase the need for internal energy storage capacity, increasing the LCOA.

This optimal tidal phasing analysis could be applied to different tidal regions around the world. The analysis could be extended by including an analysis of whether utilising tidal phasing is most useful for either grid energy, green ammonia production or other green fuel production (such as green hydrogen).

5. Conclusion

This work demonstrates the benefit of incorporating tidal stream phasing, i.e. exploiting the difference in phase of tidal stream currents in different locations, for green ammonia production around the British Isles and within the English Channel. Small regions with close-proximity tidal phasing potential and high-energy tidal potential were determined as Orkney, the North Channel of the Irish Sea, the Bristol Channel & Pembrokeshire and Alderney (Fig. 3). A genetic algorithm was used to determine the optimal turbine locations in each region to optimize the aggregate power profile. Wake effects, blockage effects, depth-constraints, turbine spacing constraints, and two different turbine types were integrated into the modelling. A MILP optimization model was used to determine the minimal LCOA in each region in 2050.

Compared to an unphased, single turbine of the same yearly CF in each region, phasing significantly reduces the LCOA (by 6–13 %, excluding cabling costs) and energy storage CAPEX (by 50–85 %) (Fig. 4). Although cabling costs are significant, particularly in Alderney (where cabling represents 38 % of the LCOA), the tidal CAPEX always contributes more than the cabling CAPEX to the LCOA (Fig. 6). However, detailed modelling of optimal cabling (length and power capacity per cable), ammonia plant location and total number of tidal turbines would be required to accurately answer in which cases the cable cost from spread-out, phased turbines is worth the phasing benefit.

Compared to the two previous papers on tidal phasing [17,21], which select the location of tidal stream turbines to optimize the aggregate power profile, this paper uses high spatial resolution tidal data and turbine locations not confined to water depths between 25 and 50 m or to specific tidal stream velocities. This paper is the first to incorporate optimal tidal phasing with green fuel production, and can be applied to any other tidal hotspot around the world (such as the Cook Inlet, Alaska [46]). Innovative energy solutions, such as the one presented hereby, are needed to meet the vast green ammonia production targets to reach net zero by 2050.

CRediT authorship contribution statement

Honora Driscoll: Writing – original draft, Software, Methodology, Formal analysis, Data curation, Conceptualization. **Nicholas Salmon:** Writing – review & editing, Software, Methodology. **Rene Bañares-Alcántara:** Writing – review & editing, Supervision, Resources, Project administration, Methodology, Conceptualization.

Data availability

The data that support the findings of this study are openly available from Marine Scotland at https://data.marine.gov.scot/dataset/scottish-shelf-model-1990-%E2%80%93-2014-climatology-version-201 [30] https://data.marine.gov.scot/dataset/pentland-firth-and-orkney-waters-climatology-102 [31] and https://marine.gov.scot/information/firth-clyde-model [33].

Funding

This work was supported by a studentship from UKRI for the first author (project reference: 2594549) and a Rhodes Trust scholarship for the second author.

Declaration of competing interest

The authors declare that they have no known competing financial interests or personal relationships that could have appeared to influence the work reported in this paper.

Acknowledgements

The use of MATLAB and its toolboxes was under an academic license.

The use of Gurobi was under a free academic license.

Appendix A. Supplementary data

Supplementary data to this article can be found online at https://doi.org/10.1016/j.renene.2024.122335.

Glossary

Abbreviation	Meaning
LCOA	Levelized cost of ammonia
CF	Capacity Factor
CAPEX	Capital cost
OPEX	Operating cost
HB	Haber-Bosch
ASU	Air separation unit
PFOW	Pentland Firth and Orkney Waters
FOC	Firth of Clyde
SSM	Scottish Shelf Model
MILP	Mixed integer linear program
ROMS	Regional Ocean Modelling System
EMEC	European Marine Energy Centre

References

[1] IRENA and AEA, Innovation outlook: renewable ammonia, International Renewable Energy Agency, Abu Dhabi, Ammonia Energy Association, Brooklyn (2022). https://www.irena.org/publications/2022/May/Innovation-Outlook-Renewable-Ammonia.
[2] N. Salmon, R. Bañares-Alcántara, Green ammonia as a spatial energy vector: a review, Sustain. Energy Fuels 5 (11) (2021) 2814–2839.
[3] I.G. Bryden, D.M. Macfarlane, The utilisation of short term energy storage with tidal current generation systems, Energy 25 (9) (2000) 893–907.
[4] A world first for Nova Innovation - the 'Holy Grail' of baseload tidal power, Nova Innovation (2018) [Online], https://www.novainnovation.com/news/news_/i/a-world-first-for-nova-innovation-the-holy-grail-of-baseload-tidal-power/. (Accessed 20 August 2023).
[5] Eday Flow Battery Project, The European Marine Energy Centre, 2023 [Online], https://www.emec.org.uk/projects/hydrogen-projects/eday-flow-battery-project/. (Accessed 21 August 2023).
[6] N. Salmon, R. Bañares-Alcántara, Impact of grid connectivity on cost and location of green ammonia production: Australia as a case study, Energy Environ. Sci. 14 (12) (2021) 6655–6671.
[7] H. Stevens, America needs clean electricity. These states show how to do it, Wash. Post (2023) [Online], https://www.washingtonpost.com/climate-environment/interactive/2023/clean-energy-electricity-sources/. (Accessed 21 August 2023).
[8] H. Driscoll, N. Salmon, R. Bañares-Alcántara, Exploiting the temporal characteristics of tidal stream power for green ammonia production, Renew. Energy (2024) 120377.
[9] A.S. Iyer, S.J. Couch, G.P. Harrison, A.R. Wallace, Variability and phasing of tidal current energy around the United Kingdom, Renew. Energy 51 (2013) 343–357.
[10] S.P. Neill, M.R. Hashemi, M.J. Lewis, Tidal energy leasing and tidal phasing, Renew. Energy 85 (2016) 580–587.
[11] J. Hardisty, Power intermittency, redundancy and tidal phasing around the United Kingdom, Geogr. J. 174 (1) (2008) 76–84.
[12] J.A. Clarke, G. Connor, A.D. Grant, C.M. Johnstone, Regulating the output characteristics of tidal current power stations to facilitate better base load matching over the lunar cycle, Renew. Energy 31 (2) (2006) 173–180.
[13] A.N. Commin, J. McClatchey, M.W.H. Davidson, S.W. Gibb, Close-proximity tidal phasing for 'firm' electricity supply, Renew. Energy 102 (2017) 380–389.
[14] D. Preziuso, G. García-Medina, R. O'Neil, Z. Yang, T. Wang, Evaluating the potential for tidal phase diversity to produce smoother power profiles, J. Mar. Sci. Eng. 8 (4) (2020) 246.
[15] P.G. Novo, Y. Kyozuka, Tidal stream energy as a potential continuous power producer: a case study for West Japan, Energy Convers. Manag. 245 (2021) 114533.
[16] G. Todeschini, et al., Medium-term variability of the UK's combined tidal energy resource for a net-zero carbon grid, Energy 238 (2022) 121990.
[17] S.P. Neill, M.R. Hashemi, M.J. Lewis, Optimal phasing of the European tidal stream resource using the greedy algorithm with penalty function, Energy 73 (2014) 997–1006.
[18] S.P. Neill, et al., Tidal range energy resource and optimization – past perspectives and future challenges, Renew. Energy 127 (2018) 763–778.
[19] A. Cornett, J. Cousineau, I. Nistor, Assessment of hydrodynamic impacts from tidal power lagoons in the Bay of Fundy, Int. J. Mar. Energy 1 (2013) 33–54.
[20] H. Driscoll, N. Salmon, R. Bañares-Alcántara, Technoeconomic evaluation of offshore green ammonia production using tidal and wind energy: a case study, Energy Sources, Part A Recover. Util. Environ. Eff. 45 (3) (2023) 7222–7244.
[21] S. Giorgi, J. Ringwood, Can tidal current energy provide base load? Energies 6 (6) (2013) 2840–2858.
[22] M. Lewis, S.P. Neill, P.E. Robins, M.R. Hashemi, Resource assessment for future generations of tidal-stream energy arrays, Energy 83 (2015) 403–415.
[23] S. Draper, T.A.A. Adcock, A.G.L. Borthwick, G.T. Houlsby, Estimate of the tidal stream power resource of the Pentland Firth, Renew. Energy 63 (2014) 650–657.
[24] Ofgem Approves Orkney Transmission Link, SSEN Transmission, 2023 [Online], https://www.ssen-transmission.co.uk/news/news–views/2023/7/ofgem-approves-orkney-transmission-link/. (Accessed 21 August 2023).
[25] D. Coles, et al., A review of the UK and British Channel Islands practical tidal stream energy resource, Proc. R. Soc. A 477 (2255) (2021) 20210469.
[26] M.A. Almoghayer, D.K. Woolf, S. Kerr, G. Davies, Integration of tidal energy into an island energy system - a case study of Orkney islands, Energy 242 (2022) 122547.
[27] Go West! an Analysis of the Energy System Benefits and Policy Implications of a More Geographically Diverse Offshore Wind Portfolio, Regen, 2022 [Online]. Available: https://www.regen.co.uk/publications/go-west/. (Accessed 18 September 2023).
[28] Land Cover Map 2021, Digimap, 2021 [Online], https://digimap.edina.ac.uk/roam/map/environment. (Accessed 5 September 2023).
[29] Chapter 3 Coverage, Protected Planet, 2020 [Online], https://livereport.protectedplanet.net/chapter-3. (Accessed 10 February 2023).
[30] M. De Dominicis, R. O'Hara Murray, J. Wolf, A. Gallego, The scottish shelf model 1990 – 2014 climatology version 2.01, Marine Scotland (2018), https://doi.org/10.7489/12037-1 [Online]. (Accessed 15 August 2023).
[31] R. O'Hara Murray, L. Campbell, Pentland Firth and Orkney waters climatology 1.02, Marine Scotland (2021), https://doi.org/10.7489/12041-1 [Online]. Available:. (Accessed 6 January 2022).
[32] R. O'Hara Murray, A. Gallego, A modelling study of the tidal stream resource of the Pentland Firth, Scotland, Renew. Energy 102 (B) (2017) 326–340.
[33] The Firth of Clyde model, Marine Scotland (2023) [Online]. Available: https://marine.gov.scot/information/firth-clyde-model. (Accessed 19 March 2023).
[34] Orbital Marine Power Ltd, Orbital O2 2MW Tidal Turbine, Kirkwall, United Kingdom, 2018. https://marine.gov.scot/sites/default/files/project_information_summary.pdf.
[35] J. Hayman, R. Starzmann, Floating Tidal Instream Energy, Sustainable Marine Energy & SCHOTTEL HYDRO, 2018 [Online], https://www.asiacleanenergyforum.org/wp-content/uploads/2018/06/Jason-Hayman-Floating-Tidal-Instream-Energy.pdf. (Accessed 4 April 2023).
[36] C. Legrand, Assessment of Tidal Energy Resource: Marine Renewable Energy Guides, European Marine Energy Centre, London, UK, 2009.
[37] T. Nishino, R.H.J. Willden, The efficiency of an array of tidal turbines partially blocking a wide channel, J. Fluid Mech. 708 (2012) 596–606.
[38] L. Zhao, L. Xue, Z. Li, J. Wang, Z. Yang, Y. Xue, Progress on offshore wind farm dynamic wake management for energy, J. Mar. Sci. Eng. 10 (10) (2022) 1395.

[39] J.K. Lundquist, K.K. DuVivier, D. Kaffine, J.M. Tomaszewski, Costs and consequences of wind turbine wake effects arising from uncoordinated wind energy development, Nat. Energy 4 (1) (2019) 26–34.
[40] R. Vennell, S.W. Funke, S. Draper, C. Stevens, T. Divett, Designing large arrays of tidal turbines: a synthesis and review, Renew. Sustain. Energy Rev. 41 (2015) 454–472.
[41] T.A.A. Adcock, S. Draper, R.H.J. Willden, C.R. Vogel, The fluid mechanics of tidal stream energy conversion, Annu. Rev. Fluid Mech. 53 (2021) 287–310.
[42] P. Stansby, T. Stallard, Fast optimisation of tidal stream turbine positions for power generation in small arrays with low blockage based on superposition of self-similar far-wake velocity deficit profiles, Renew. Energy 92 (2016) 366–375.
[43] Black & Veatch, Lessons Learnt from MeyGen Phase 1A Final Summary Report, 2020. Surrey, UK, https://webassets.bv.com/2020-06/MeyGen.Lessons.Learnt.Full.Report_0.pdf.
[44] T.A.A. Adcock, S. Draper, G.T. Houlsby, A.G.L. Borthwick, S. Serhadlıoğlu, The available power from tidal stream turbines in the Pentland Firth, Proc. R. Soc. A Math. Phys. Eng. Sci. 469 (2157) (2013) 20130072.
[45] M. De Dominicis, R. O'Hara Murray, J. Wolf, Multi-scale ocean response to a large tidal stream turbine array, Renew. Energy 114 (2017) 1160–1179.
[46] T. Wang, Z. Yang, A tidal hydrodynamic model for Cook inlet, Alaska, to support tidal energy resource characterization, J. Mar. Sci. Eng. 8 (4) (2020) 254.